JACS
JOURNAL OF THE AMERICAN CHEMICAL SOCIETY
Communication
pubs.acs.org/JACS

Leukocyte-Mimicking Stem Cell Delivery via in Situ Coating of Cells with a Bioactive Hyperbranched Polyglycerol

Jae Hyun Jeong,[†,#] John J. Schmidt,[†,∥,#] Richie E. Kohman,[‡,#] Andrew T. Zill,[‡] Ross J. DeVolder,[†] Cartney E. Smith,[†] Mei-Hsiu Lai,[†] Artem Shkumatov,[†,∥] Tor W. Jensen,[⊥] Lawrence G. Schook,[§] Steven C. Zimmerman,[‡] and Hyunjoon Kong*[,†,∥]

[†]Department of Chemical and Biomolecular Engineering, [‡]Department of Chemistry, [§]Department of Animal Sciences, [∥]Institute for Genomic Biology, and [⊥]Division of Biomedical Sciences, University of Illinois at Urbana-Champaign, Urbana, Illinois 61801, United States

Supporting Information

ABSTRACT: Since stem cells emerged as a new generation of medicine, there are increasing efforts to deliver stem cells to a target tissue via intravascular injection. However, the therapeutic stem cells lack the capacity to detect and adhere to the target tissue. Therefore, this study presents synthesis of a bioactive hyperbranched polyglycerol (HPG) that can noninvasively associate with stem cells and further guide them to target sites, such as inflamed endothelium. The overall process is analogous to the way in which leukocytes are mobilized to the injured endothelium.

Stem and progenitor cells are being extensively studied as a new generation of medical therapy because of their ability to produce therapeutic proteins and recreate new tissues sustainably.[1−5] One popular cell transplantation strategy is to inject cells into the circulatory system. However, this approach often encounters difficulties in recruiting transplanted cells to the target tissue because therapeutic cells, such as mesenchymal stem cells, lack the capability to bind with the target tissue. According to fundamental studies, leukocytes are mobilized to injured or pathologic tissues because they express transmembrane receptors that can specifically bind with proteins overexpressed by the tissue. To mimic the function of leukocytes, efforts are increasingly being made to modify the therapeutic cell surface with peptides or antibodies that can associate with proteins overexpressed in target tissues.[6,7] For example, the cell surface was first modified with protein linkers such as protein G using activated esters or thiol maleimides and subsequently exposed to intercellular adhesion molecule (ICAM) antibodies or E-selectin binding peptides;[8−11] however, such sequential and chemical modification of the cell surface may negatively impact the cell viability and therapeutic activity. Such concerns were not well-addressed in these past studies.

Therefore, this study presents a nanosized cell carrier that can noninvasively modify cell surfaces with vasculature binding peptides (VBPs) via in situ self-assembly with cells and regular cellular anchorage to target tissues (Scheme 1). In this study, we hypothesized that hyperbranched polyglycerol (HPG) covalently modified with octadecyl chains and VBPs would bind with cell membranes through hydrophobic chain insertion

Scheme 1. A Bioactive Hyperbranched Polyglycerol (HPG) Covalently Modified with Octadecyl Chains and Vasculature Binding Peptides (VBPs) Was Utilized as a Novel Cell-Guidance Molecule That Can Associate with Stem Cells and Further Guide Them to Target Defective Vasculature

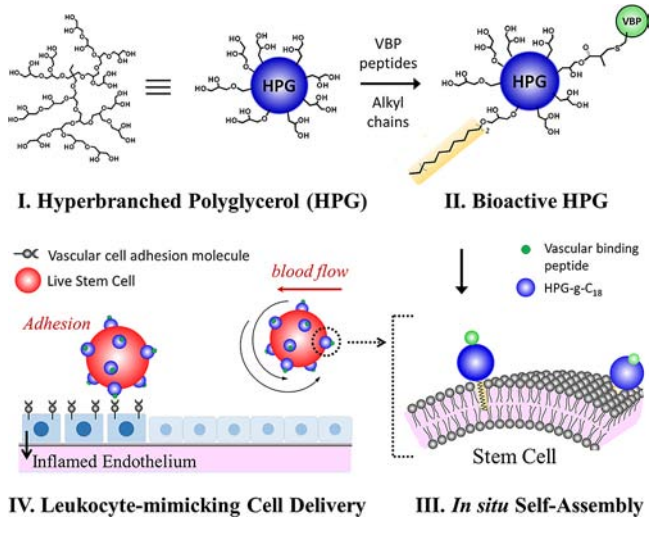

and display a controlled number of VBPs on the cell surface (I−III in Scheme 1). Additionally, the number of VBP-conjugated HPGs on the cell membrane would control the adhesion of transplanted cells to the target tissue (IV in Scheme 1). The HPG possesses a compact, globular architecture that has a restricted conformation, minimizing intermolecular entanglements often encountered with linear polymers.[12−18] Such a molecular architecture is more advantageous for presenting a larger number of octadecyl chains and VBPs than linear polymers.[19]

Additionally, the HPG consisting of polyether−polyol units is highly water-soluble and minimally stimulates host responses (i.e., it exhibits high biocompatibility).[20−22] The number of octadecyl chains linked to the HPG would tune the binding affinity between the HPG and cells. In this study, an oligopeptide containing the VHSPNKK sequence was used as

Received: January 25, 2013
Published: April 16, 2013

   dx.doi.org/10.1021/ja400636d | J. Am. Chem. Soc. 2013, 135, 8770−8773

a model VBP because it is known to bind with vascular endothelial adhesion molecule (VCAM) overexpressed by inflamed blood vessels.[23,26] We evaluated the association and dissociation kinetics of the biofunctionalized HPG on the VCAM-coated substrate using surface plasmon resonance (SPR) spectroscopy. We also used an in vitro circulation system to demonstrate that the resulting biofunctionalized HPG associates with mesenchymal stem cells (MSCs) and guides them to inflammatory tissue.

First, to develop an HPG capable of binding cell surfaces, HPG-*g*-C_{18} was prepared by treating a 150 kDa HPG with octadecyl bromide (C_{18}–Br) and base [Figure S1a in the Supporting Information (SI)]. ^{1}H NMR analysis indicated that an average of seven C_{18} chains was linked per HPG (Figure S1b; see eq 1 in the SI). The resulting HPG-*g*-C_{18} remained soluble in water and could be readily dissolved in cell suspensions. The capability of HPG-*g*-C_{18} to associate with cells was evaluated by using SPR spectroscopy to measure an association rate constant (k_a), a dissociation rate constant (k_d), and the number of HPG-*g*-C_{18} that adhered to a lipid bilayer simulating a cell membrane.[24,25] Both k_a and k_d were quantified by fitting SPR curves to 1:1 Langmuir model using eq 1,

$$\frac{dRU}{dt} = k_a[A](RU_{max} - RU) - k_dRU \quad (1)$$

where RU_{max} is the maximum value of the response unit (RU) when the target surface is saturated with HPG-*g*-C_{18} and [A] is the HPG-*g*-C_{18} concentration. As expected, HPG-*g*-C_{18} exhibited a higher RU change (ΔRU) and k_a and a smaller k_d than the unmodified HPG (Table 1 and Figure S2a). Additionally, HPG-*g*-C_{18} conjugated with fluorescein displayed a limited increase of ΔRU relative to nonfluorescent HPG-*g*-C_{18}.

Table 1. SPR Response Unit Changes (ΔRU) and Calculated Surface Densities of Unmodified HPG and HPG-*g*-C_{18} on the Lipid Bilayer

carrier	ΔRU[a]	surface density (ng/mm^2)[b]	surface HPG number density (mm^{-2})[c]
HPG	180	0.18	7.2×10^8
HPG-*g*-C_{18}	1900	1.9	7.5×10^9

[a]Response unit change due to the binding of HPG on the lipid bilayer. [b]Calculated from the response unit (RU). [c]Calculated from the RU and the weight-average molecular weight (M_w) of the HPG (150 kDa) on the lipid bilayer.

Additionally, the underlying mechanism by which the C_{18} chains improve the association of HPG with the cell membrane was examined by quantifying the standard enthalpy (ΔH°), entropy (ΔS°), and Gibbs free energy (ΔG°).[27] The measured K_A for association of HPG-*g*-C_{18} with the cell membrane decreased with increasing temperature (Table 2). The values of ΔG° calculated from eq 2,

$$\Delta G^\circ = -RT \ln(K_A) \quad (2)$$

were approximately −11 kcal/mol. The ΔH° and ΔS° values were determined using the van't Hoff equation (eq 3),

$$-\ln(K_A) = \left(\frac{\Delta H^\circ}{R}\right)\left(\frac{1}{T}\right) - \frac{\Delta S^\circ}{R} \quad (3)$$

Table 2. Quantified Analysis of the Effect of Temperature on the Association Rate Constant (k_a), Dissociation Rate Constant (k_d), and Affinity Constant (K_A) of HPG-*g*-C_{18} toward the Lipid Bilayer

T (K)	conc. (mg/mL)	ΔRU	k_d (10^{-4} s^{-1})	k_a (10^4 M^{-1} s^{-1})	K_A (10^7 M^{-1})
298	0.05	1900	3.98	3.03	7.6
303	0.05	1300	4.73	2.37	5.0
310	0.05	780	9.79	2.92	3.0

which indicates that a plot of $-\ln(K_A)$ versus $1/T$ should be linear with a slope and *y*-intercept related to ΔH° and ΔS°, respectively. The plot of $-\ln(K_A)$ versus $1/T$ was fit using linear regression (Figure S3), and the ΔH° and ΔS° values were found to be −14.2 kcal/mol and −11.6 cal mol^{-1} K^{-1}, respectively. These results indicate that the thermodynamically favorable association between HPG-*g*-C_{18} and the lipid membrane is driven by the negative enthalpy.

Furthermore, mixing HPG-*g*-C_{18} with CD44/CD90-positive and CD45-negative MSCs resulted in the coating of MSCs with HPGs after a 10 min period. Thus, fluorescein-conjugated HPG-*g*-C_{18} was observed to stain the cell surface, whereas MSCs mixed with unmodified HPG exhibited minimal fluorescence (Figure S4). The fluorescence intensity on the cell surface minimally changed over 72 h, indicating a long residence time for the HPG-*g*-C_{18} attached to the cell membrane (Figure S4). The MSCs associated with HPG-*g*-C_{18} displayed a minimal difference in metabolic activity compared to uncoated cells (Figure S5).

Next, to target damaged tissue, HPG-*g*-C_{18} was modified with a VCAM-binding peptide containing the VHSPNKK sequence, termed VHSPNKK peptide. For the peptide conjugation, certain hydroxyl groups of HPG-*g*-C_{18} were modified to present acrylate groups (Figure 1a). These Michael acceptor groups could be conjugated to the thiol group of the VHSPNKK peptide upon treatment with base. From the UV absorbance of the tryptophan residue of the VHSPNKK peptide, it was found that HPG-*g*-C_{18} contained on average 10 peptide groups per alkyl group.

The capability of the VHSPNKK–HPG-*g*-C_{18} to bind with a VCAM-coated substrate was evaluated using SPR spectroscopy. As expected, the unmodified HPG-*g*-C_{18} displayed minimal adhesion to the substrate, as indicated by the value of ΔRU (Figure 1b). In contrast, VHSPNKK–HPG-*g*-C_{18} exhibited an affinity constant 6-fold larger than that of the peptide-free HPG-*g*-C_{18}. Accordingly, the number of VHSPNKK–HPG-*g*-C_{18} bound to the VCAM-coated substrate, represented by ΔRU, increased in proportion to the number of HPG molecules added to the SPR unit. Ultimately, the number of peptide-conjugated HPG-*g*-C_{18} bound to the VCAM substrate was 10 times larger than the number of peptide-free HPG-*g*-C_{18} after a 300 s time period (Figure 1c). However, VHSPNKK–HPG-*g*-C_{18} exhibited minimal adhesion to a substrate pre-exposed to free VSHPNKK peptide (Figure S6). Taken together, these results indicate that the VHSPNKK peptide plays a critical role in the targeted adhesion of HPG to the VCAM-coated substrate.

Finally, we used SPR spectroscopy to examine the ability of VHSPNKK–HPG-*g*-C_{18} to guide MSCs to a target VCAM-coated substrate (Figure 2a). Interestingly, MSCs coated with VHSPNKK–HPG-*g*-C_{18} displayed a 1.5-fold increase in k_a and a 70% decrease in k_d compared with uncoated MSCs (Figures

dx.doi.org/10.1021/ja400636d | J. Am. Chem. Soc. 2013, 135, 8770–8773

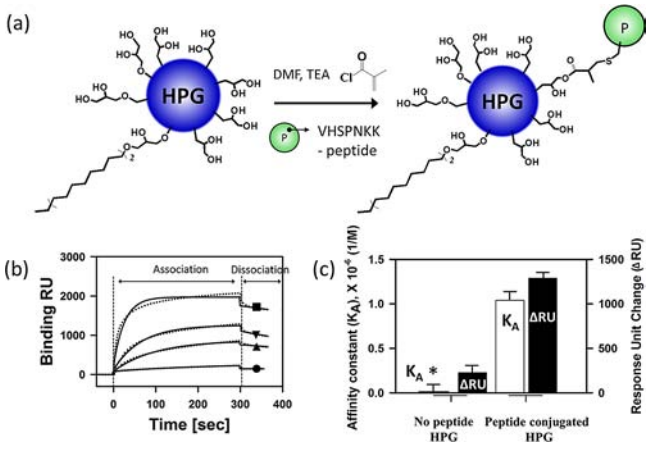

Figure 1. Bioconjugation of HPG-*g*-C_{18} with VHSPNKK peptides and SPR analysis of the binding of VHSPNKK−HPG-*g*-C_{18} with VCAM. (a) Chemical reaction scheme for conjugation of HPG-*g*-C_{18} with VHSPNKK peptide. (b) SPR response curves for VHSPNKK−HPG-*g*-C_{18}'s association with and dissociation from the VCAM-coated substrate. (c) SPR analysis of the affinity constant (K_A) and response unit change (ΔRU) of VHSPNKK−HPG-*g*-C_{18} for the VCAM-coated substrate. In (b), -●- represents peptide-free polyglycerol at 5.0 μM concentration. The concentration of VHSPNKK−HPG-*g*-C_{18} incorporated into the flow of the SPR unit was varied from 1.2 (-▲-) to 5.0 (-▼-) to 10 μM (-■-). The dotted lines show the binding RUs obtained. The solid lines represent global fits to a 1:1 Langmuir model (A + B ⇄ AB). The scores of χ^2 at 1.2 and 5.0 μM were <10, indicating that the model used adequately describes the observed binding.

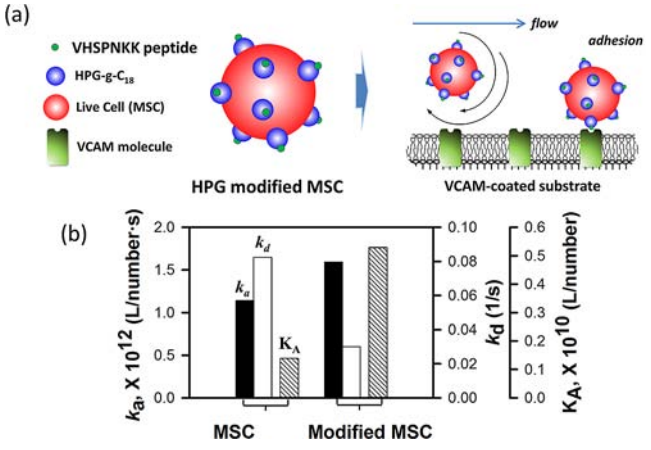

Figure 2. In vitro evaluation of the function of VHSPNKK−HPG-*g*-C_{18} to regulate adhesion of MSCs to an inflamed endothelium. (a) Schematic of the SPR analysis to characterize adhesion of MSCs to a target VCAM-coated substrate. (b) Association rate constant (k_a), dissociation rate constant (k_d), and affinity constant (K_A) of uncoated MSCs and MSCs associated with VHSPNKK−HPG-*g*-C_{18}, as determined from SPR response curves.

2b and S7). Additionally, the affinity constant for MSCs associated with VHSPNKK−HPG-*g*-C_{18} was 3 times larger than the K_A value for uncoated MSCs.

Furthermore, we examined the ability of VHSPNKK−HPG-*g*-C_{18} to direct the adhesion of CD44/CD90-positive and CD45-negative adipose-derived MSCs to an inflamed endothelium using a blood-vessel-mimicking circulation system (Figures 3a and S8). The inflamed endothelium was prepared by exposing an endothelial cell sheet to tumor necrosis factor α

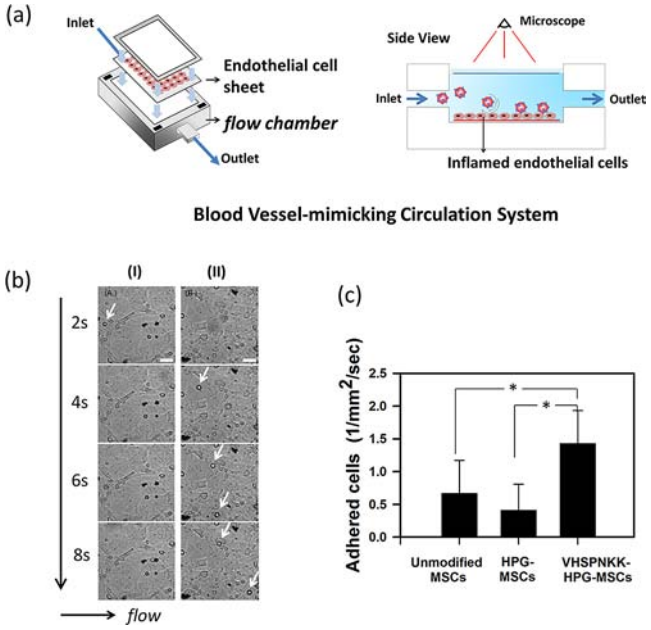

Figure 3. In vitro evaluation of the function of VHSPNKK−HPG-*g*-C_{18} to regulate adhesion of MSCs to an inflamed endothelium. (a) Schematic of the MSC delivery to a target inflamed endothelium using an in vitro circulation system. (b) Images of the inflamed endothelial cells exposed to the flow of (I) uncoated MSCs and (II) MSCs associated with VHSPNKK−HPG-*g*-C_{18}. Arrows indicate MSCs anchored to the endothelial cells. The scale bar represents 50 μm. (c) Quantification of the number of MSCs adhered to the target inflamed endothelial cells during a given time period. * represents a statistical significance of the difference between conditions ($P < 0.05$).

(TNF-α), which induced endothelial cells to overexpress VCAM.[28] The flow rate of MSC-suspending fluid was kept constant at 1.0 mL/min in order to keep the shear stress on the endothelium comparable to coronary artery wall shear stress. Both uncoated MSCs and MSCs associated with peptide-free HPG-*g*-C_{18} displayed minimal cell adhesion to the inflamed cells (Figure 3b and movie 1 in the SI). In contrast, MSCs coated with VHSPNKK−HPG-*g*-C_{18} displayed significantly smaller rolling velocities compared with uncoated cells and actively adhered to the inflamed endothelium (Figures 3b and S9 and movie 2 in the SI). Sphere-shaped MSCs with a 10 μm diameter were readily distinguished from any debris in the cell culture medium and endothelial cells fully spread on a substrate. Ultimately, there was a 2-fold increase in the number of MSCs adhered to the endothelium when VSPNKK-HPG-*g*-C_{18} was used (Figure 3c). In addition, the MSCs associated with VHSPNKK−HPG-*g*-C_{18} molecules displayed limited adhesion to endothelial cells not exposed to TNF-α. These results support the finding that the peptide-conjugated HPGs are capable of delivering cells exclusively to the target inflammatory tissue.

In summary, this study demonstrates a novel cell-guidance molecule that can associate with cells in a minimally invasive manner and further guide them to target sites, such as inflamed endothelium. HPGs modified with octadecyl chains associated with MSCs in a thermodynamically favorable manner. Subsequent modification of HPG-*g*-C_{18} with VHSPNKK peptides provided HPG molecules with the ability to bind with VCAM-coated substrate. Ultimately, coating stem cell surfaces with VHSPNKK−HPG-*g*-C_{18} significantly enhanced the cellular affinity for the VCAM protein and therefore

dx.doi.org/10.1021/ja400636d | *J. Am. Chem. Soc.* 2013, 135, 8770−8773

successfully directed the anchorage of cells to the target inflamed endothelium. The overall process is analogous to the way in which leukocytes are mobilized to the injured endothelium.[29] Additionally, this approach to functionalization of the cell membrane with VHSPNKK−HPG-*g*-C_{18} via self-assembly should be superior to prior, multistep chemical modifications of cell membranes.

We envisage that the strategy described herein, using an HPG carrier to bind cells and display targeting groups for delivery, will be highly useful for guiding a wide array of therapeutic cells to target tissues following intravascular injection. Such enhanced cell adhesion and subsequent increased cell quantities at target tissues should greatly improve the outcome of cell therapies. In addition, this functionalized HPG may prove useful for guiding various nano- or microsized drug carriers to target tissues. These possibilities are the focus of our current studies.

■ ASSOCIATED CONTENT

Supporting Information

Experimental materials, instruments, and procedures; synthesis and characterization of VHSPNKK−HPG-*g*-C_{18}; analysis of the association of HPG-*g*-C_{18} with cells; SPR analysis and flow chamber assay; and supplemental videos for the adhesion of modified MSCs to an inflamed endothelium. This material is available free of charge via the Internet at http://pubs.acs.org.

■ AUTHOR INFORMATION

Corresponding Author

hjkong06@illinois.edu

Author Contributions

[#]J.H.J., J.J.S., and R.E.K. contributed equally.

Notes

The authors declare no competing financial interest.

■ ACKNOWLEDGMENTS

This work was supported by the National Institutes of Health (1R21 HL097314 and 1R01 HL109192 to H.K. and S.C.Z. and 1R25CA154015A to R.J.D.). We also acknowledge the Biomedical Research Center, a joint venture of Carle Foundation Hospital and the University of Illinois at Urbana-Champaign, for services provided in support of this research.

■ REFERENCES

(1) Asahara, T.; Kawamoto, A. *Am. J. Physiol.: Cell Physiol.* **2004**, *287*, 572−579.
(2) Kinnaird, T.; Stabile, E.; Burnett, M. S.; Epstein, S. E. *Circ. Res.* **2004**, *95*, 354−363.
(3) Minguell, J. J.; Erices, A. *Exp. Biol. Med.* **2006**, *231*, 39−49.
(4) Perin, E. C.; Geng, Y. J.; Willerson, J. T. *Circulation* **2003**, *107*, 935−938.
(5) Shah, B. S.; Clark, P. A.; Moioli, M. A.; Stroscio, M. A.; Mao, J. J. *Nano Lett.* **2007**, *7*, 3071−3079.
(6) Ko, I. K.; Kean, T. J.; Dennis, J. E. *Biomaterials* **2009**, *30*, 3702−3710.
(7) Sarkar, D.; Vemula, P. K.; Zhao, W.; Gupta, A.; Karnik, R.; Karp, J. M. *Biomaterials* **2010**, *31*, 5266−5271.
(8) Behm, C. Z.; Kaufmann, B. A.; Carr, C.; Lankford, M.; Sanders, J. M.; Rose, C. E.; Kaul, S.; Lindner, J. R. *Circulation* **2008**, *117*, 2902−2911.
(9) Sakhalar, H. S.; Dalal, M. K.; Salem, A. K.; Ansari, R.; Fu, J.; Kiani, M. F.; Kurjiaka, D. T.; Hanes, J.; Shakesheff, K. M.; Goetz, D. J. *Proc. Natl. Acad. Sci. U.S.A.* **2003**, *100*, 15895−15900.
(10) Dickerson, J. B.; Blackwell, J. E.; Ou, J. J.; Shinde Patil, V. R.; Goetz, D. J. *Biotechnol. Bioeng.* **2001**, *73*, 500−509.
(11) (a) Eniola, A. O.; Rodgers, S. D.; Hammer, D. A. *Biomaterials* **2002**, *23*, 2167−2177. (b) Sarkar, D.; Spencer, J. A.; Phillips, J. A.; Zhao, W.; Schaefer, S.; Spelke, D. P.; Mortensen, L. J.; Ruiz, J. P.; Vemula, P. K.; Sridharan, R.; Kumar, S.; Karnik, R.; Lin, C. P.; Karp, J. M. *Blood* **2011**, *118*, e184−e191.
(12) Sunder, A.; Hanselmann, R.; Frey, H.; Mülhaupt, R. *Macromolecules* **1999**, *32*, 4240−4246.
(13) Sunder, A.; Mülhaupt, R.; Haag, R.; Frey, H. *Macromolecules* **2000**, *33*, 253−254.
(14) Mumprecht, S.; Schurch, C.; Schwaller, J.; Solenthaler, M.; Ochsenbein, A. F. *Blood* **2009**, *114*, 1528−1536.
(15) Vellai, T.; Takacs-Vellai, K. *Adv. Exp. Med. Biol.* **2010**, *694*, 69−80.
(16) Stephan, M. T.; Irvine, D. J. *Nano Today* **2011**, *6*, 309−325.
(17) Zimmerman, S. C.; Quinn, J. R.; Burakowska, E.; Haag, R. *Angew. Chem., Int. Ed.* **2007**, *46*, 8164−8167.
(18) (a) Sisson, A. L.; Steinhilber, D.; Rossow, T.; Welker, P.; Licha, K.; Haag, R. *Angew. Chem., Int. Ed.* **2009**, *48*, 7540−7545. (b) Wei, T.; Yong, L.; Binbin, J.; Songrui, Y.; Wei, H.; Yongfeng, Z.; Deyue, Y. *J. Am. Chem. Soc.* **2012**, *134*, 762−764.
(19) Wilms, D.; Stiriba, S. E.; Frey, H. *Acc. Chem. Res.* **2010**, *43*, 129−141.
(20) Kainthan, R. K.; Janzen, J.; Levin, E.; Devine, D. V.; Brooks, D. E. *Biomacromolecules* **2006**, *7*, 703−709.
(21) Kainthan, R. K.; Hester, S. R.; Levin, E.; Devine, D. V.; Brooks, D. E. *Biomaterials* **2007**, *28*, 4581−4590.
(22) Kelly, K. A.; Allport, J. R.; Tsourkas, A.; Shinde-Patil, V. R.; Josephson, L.; Weissleder, R. *Circ. Res.* **2005**, *18*, 327−336.
(23) Stabenfeldt, S. E.; Gossett, J. J.; Barker, T. H. *Blood* **2010**, *116*, 1352−1359.
(24) (a) Kim, B. Y.; Jeong, J. H.; Park, K.; Kim, J. D. *J. Controlled Release* **2005**, *102*, 525−538. (b) Jeong, J. H.; Kim, B. Y.; Lee, S. J.; Kim, J. D. *Chem. Phys. Lett.* **2006**, *421*, 373−377.
(25) Lai, M. H.; Jeong, J. H.; DeVolder, R. J.; Brockman, C.; Schroeder, C.; Kong, H. J. *Adv. Funct. Mater.* **2012**, *22*, 3239−3246.
(26) Chou, C. C.; Hsiao, H. Y.; Hong, Q. S.; Chen, C. H.; Peng, Y. W.; Chen, H. W.; Yang, P. C. *Nano Lett.* **2008**, *8*, 437−445.
(27) Day, Y. S. N.; Baird, C. L.; Rich, R. L.; Myszka, D. G. *Protein Sci.* **2002**, *11*, 1017−1025.
(28) Lee, C. W.; Lin, W. N.; Lin, C. C.; Luo, S. F.; Wang, J. S.; Pouyssegur, J.; Yang, C. M. *J. Cell Physiol.* **2006**, *207*, 174−186.
(29) Elices, M. J.; Osborn, L.; Takada, Y.; Crouse, C.; Luhowskyj, S.; Hemler, M. E.; Lobb, R. R. *Cell* **1990**, *23*, 577−584.